Pergamon

Int. J. Heat Mass Transfer. Vol. 39, No. 8, pp. 1677–1686, 1996

0017-9310/96 $15.00 + 0.00

0017-9310(95)00254-5

Improving the performance of adsorption heat exchangers using a finned structure

A. HAJJI

Département de Génie Industriel Alimentaire, Institut Agronomique et Vétérinaire Hassan II, B.P. 6202 Rabat-Instituts, Morocco

and

S. KHALLOUFI

AGA-Ingénierie, Secteur 10 lot 28 Ilot No 1, Avenue Annakhil Hayt Ryad, Rabat, Morocco

(*Received* 27 *February* 1995 *and in final form* 27 *June* 1995)

Abstract—This paper presents a numerical investigation of the sorption kinetics under constant-pressure conditions using a finned adorption reactor. The governing equations, derived from local thermodynamic equilibrium and energy balance, are solved using an explicit scheme. The model is validated and used to analyze the effect of important design parameters on the performance of the adsorbent reactor. It is found that using metallic fins at sufficiently small intervals and reducing the contact resistance at the interface, metal-adsorbent can improve significantly sorption kinetics. However, the fin thickness and the nature of the metal have little effect on the rate of heat transfer. The model can be used to optimize the design of efficient adsorption heat exchangers.

INTRODUCTION

Significant progress has been achieved during the last two decades in the development of adsorption cooling and heating systems considered as a serious alternative to vapor compression [1]. A detailed description of the operating principle and thermodynamic analysis of solid sorption refrigeration machines is given in ref. [2]. Applications of adsorption systems include solar cooling, energy storage, automobile and residential space conditioning... etc. [3–5]. The state-of-the-art in adsorption technology is discussed in a recent publication of the International Institute of Refrigeration [6].

The efficiency of an adsorption system is characterized by the coefficient of performance (COP) and the specific power ratio (SPR) expressed as the cooling or heating output per unit mass or volume of adsorbent material. The COP and the SPR are critical for cost effective machines as they are directly related to the running and investment costs, respectively. Various studies have shown that the COP and the SPR can both be improved by using energy recovery techniques [7, 8] or increasing sorption kinetics [9, 10]. The limiting factor of low adsorbent thermal conductivity is overcome by classical heat transfer enhancement techniques, such as using composite materials [11, 12] or metallic matrix structures [13], reducing the contact resistance between the adsorbent and the external heating/cooling fluid [14], minimizing the adsorbent thickness [15] and using compact heat exchangers of improved design [16, 17].

The key component in an adsorption system is the adsorbent reactor, which is a heat exchanging device between the cooling/heating fluid and the adsorbent material. Therefore, the proper design of adsorption machines requires a good understanding of the simultaneous heat and mass transfer occurring in these devices. Relatively few published studies deal with these important aspects, as major effects concentrate on the development and testing of prototypes designed by the methods of heat exchangers theory. In ref. [18], formulas which describe both constant-volume and constant-pressure adsorption processes are derived from thermodynamic analysis. Basic experimental and theoretical investigation of these processes which compose adsorption cycles are presented in refs. [19, 10].

This paper presents a numerical investigation of the improvement in sorption kinetics under constant-pressure conditions. The objective is to develop a theoretical model allowing an accurate analysis of the effect of important design parameters on sorption kinetics and on the behavior of adsorption cooling machines. In Section 2, the governing equations are derived from local energy balance and thermodynamic equilibrium conditions. Section 3 presents the numerical solution and its validation by comparison to other results. Section 4 discusses the influence on sorption kinetics of such parameters as the distance between the fins, the contact resistance

NOMENCLATURE

$A(W)$ polynomial function introduced in equation (2)
$B(W)$ polynomial function introduced in equation (2)
C specific heat [J kg^{-1} K^{-1}]
C_{ap} apparent specific heat defined in equation (5) [J kg^{-1} K^{-1}]
$C_1 \ldots C_7$ constant defined in equations (26–28)
E_m fin thickness [m]
E_s half the thickness of adsorbent layer [m]
G adsorptivity defined in equation (4) [kg adsorbates kg adsorbent^{-1} K^{-1}]
k thermal conductivity [W m^{-1} K^{-1}]
L half the distance between the fins [m]
P_v adsorbate vapor pressure [mbar]
R_c contact resistance [m^2 K W^{-1}]
t time [s]
T temperature [°C]
x, y space coordinates
W uptake [kg of adsorbate kg of adsorbent^{-1}].

Greek symbols
ΔH heat of sorption [J kg^{-1}]
$\Delta x, \Delta y, \Delta t$ space and time steps [m]
$\Delta\zeta, \Delta\eta, \Delta\tau$ dimensionless space and time steps defined in equation (25)
κ dimensionless thermal conductivity defined in equation (23)
ζ, η, τ dimensionless space and time coordinate defined in equation (24)
θ dimensionless temperature defined in equation (23)
ρ mass density [kg m^{-3}]
ξ dimensionless apparent specific heat defined in equation (23).

Subscripts
a adsorbate
ave average
co condensation
m metallic fin
o initial (at time 0)
s adsorbent
∞ heating/cooling medium.

between the metallic parts and the adsorbent material, the fin thickness and the nature of the metal.

THEORETICAL ANALYSIS

Figure 1 shows the geometry of the finned adsorption reactor, assumed to be of parallelipedic shape. The adsorbent material of thickness E_s is heated/cooled symmetrically from its upper and lower sides by a fluid at temperature T_∞. In order to enhance sorption kinetics, metallic fins of thickness $2E_m$ are inserted into the adsorbent material at a distance $2L$. Taking into account the symmetry of the system, the study will be limited to the element shown in Fig. 2.

In order to simplify the analysis, the following assumptions are made: (i) the length in the z-direction is much larger than the other dimensions, therefore relevant properties are assumed to depend only on x and y coordinates. (ii) The fin temperature is a function of the y-coordinate. (iii) The temperature of the

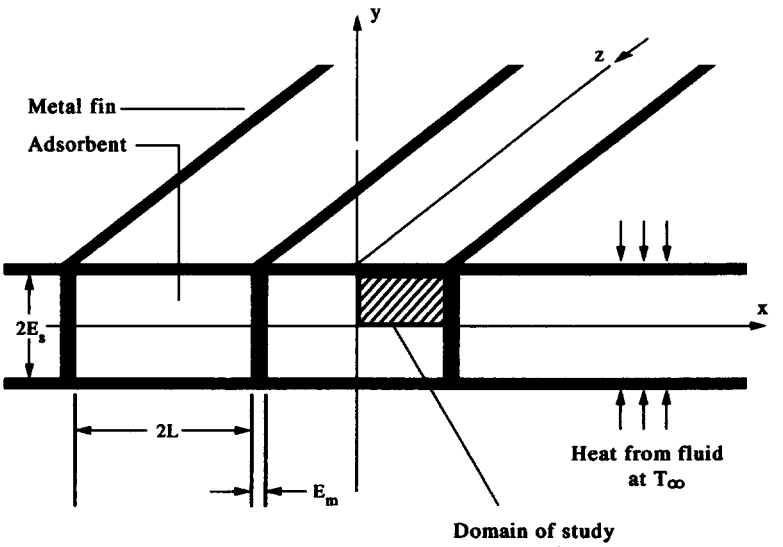

Fig. 1. Schematic representation of a finned adsorption reactor.

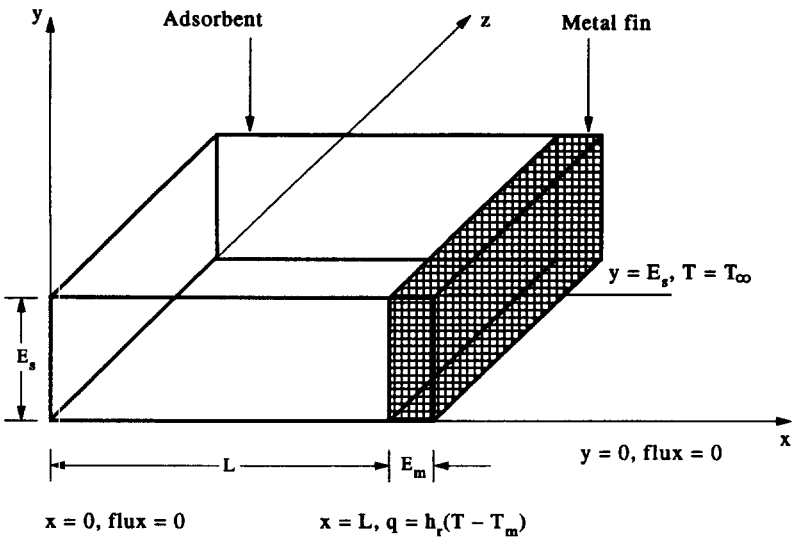

Fig. 2. The domain of study.

heating/cooling fluid is constant. (iv) Contact resistance between either the walls of the heat exchanger or the fins and the adsorbent is taken as the inverse of a heat transfer coefficient h_c. (v) The pressure of the vapor phase is uniform through the adsorbent thickness and remains constant. (vi) Thermodynamic equilibrium holds at all times. (vii) Thermal conductivity and specific heat of the metal are constant and those of the adsorbent vary linearly with the uptake. The validity of these assumptions is discussed in previous publications [10, 19].

The isotherm equation

The state of an adsorption system is characterized by three state properties the temperature T, the uptake W and the vapor pressure P_v of the adsorbate. Under thermodynamic equilibrium these parameters T, W and P_v satisfy the isotherm equation

$$\ln(P_v) = F(T, W). \tag{1}$$

For the pair Zeolite 4A-water considered in this study the sorption data are well fitted by the following relationship:

$$\ln(P_v) = A(W) + \frac{B(W)}{T}. \tag{2}$$

$A(W)$ and $B(W)$ are third-order polynomials with coefficients $A_0 = 14.8979$, $A_1 = 95.4083$, $A_2 = -636.658$, $A_3 = 1848.84$, $B_0 = -7698.85$, $B_1 = 21{,}498.1$, $B_2 = -184{,}598.0$, $B_3 = 512{,}605.0$. During a constant-pressure process, isotherm equation (1) imposes a nonlinear relation between T and W represented in Fig. 3.

Adsorbent temperature distribution

Since we consider constant-pressure processes, the pressure is fixed and the assumption of thermodynamic equilibrium implies that the isotherm equation gives a relationship between T and W. Therefore, we need only solve for the temperature distribution in order to determine the state of the adsorbent material at each point. The following partial differential equation can be derived by writing the energy balance of a differential element of adsorbent material:

$$\rho_s(C_s + WC_a)\frac{\partial T}{\partial t} = \frac{\partial}{\partial x}\left(k\frac{\partial T}{\partial x}\right) + \frac{\partial}{\partial y}\left(k\frac{\partial T}{\partial y}\right) + \rho_s \Delta H \frac{\partial W}{\partial t}. \tag{3}$$

The terms in the left hand side (LHS) correspond to the sensible heats gained, respectively, by the adsorbent and the adsorbate phase. The first two terms in the right hand side (RHS) correspond to the conductive heat fluxes and the last term is the latent heat of sorption which is proportional to the uptake variation. Introducing the apparent specific heat and the adsorptivity defined as

$$G(T, W) = -\frac{\partial W}{\partial T} \tag{4}$$

$$C_{ap}(T, W) = C_s + WC_a + G(T, W)\Delta H \tag{5}$$

a more convenient form of equation (3) is obtained

$$\rho_s C_{ap}\frac{\partial T}{\partial t} = \frac{\partial}{\partial x}\left(k\frac{\partial T}{\partial x}\right) + \frac{\partial}{\partial y}\left(k\frac{\partial T}{\partial y}\right). \tag{6}$$

This equation is valid for $0 < y < E_s$, $0 < x < L$ and $t > 0$. The boundary conditions express the symmetry conditions and heat transfer between the metal and the adsorbent:

(a) on the symmetry x-axis ($y = 0$)

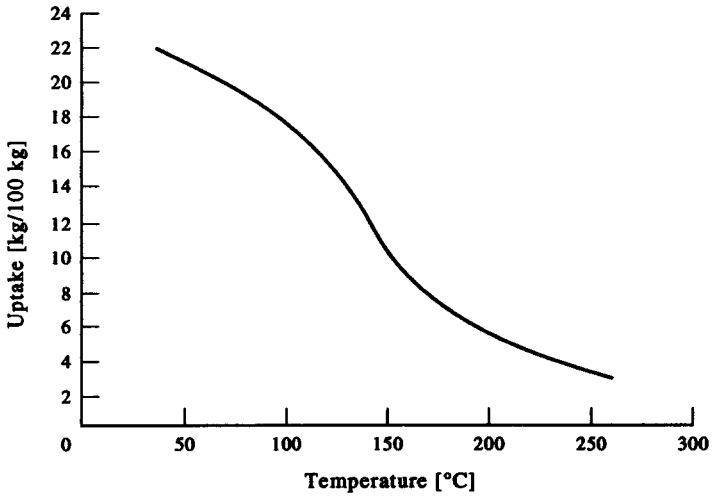

Fig. 3. Uptake variation with temperature at constant-pressure (adsorption pair = Zeolite 4A-water, $T_{co} = 30°C$).

$$\frac{\partial T}{\partial y} = 0 \quad \text{for} \quad y = 0 \quad 0 < x < L \quad t > 0; \quad (7)$$

(b) at the interface metal-adsorbent ($y = E_s$)

$$k\frac{\partial T}{\partial y} = (1/R_c)(T_\infty - T)$$

$$\text{for} \quad y = E_s \quad 0 < x < L \quad t > 0; \quad (8)$$

(c) on the symmetry y-axis ($x = 0$)

$$\frac{\partial T}{\partial x} = 0 \quad \text{for} \quad x = 0 \quad 0 < y < E_s \quad t > 0; \quad (9)$$

(d) at the interface fin-adsorbent ($x = L$)

$$k\frac{\partial T}{\partial x} = (1/R_c)(T_m - T)$$

$$\text{for} \quad x = L \quad 0 < y < E_s \quad t > 0. \quad (10)$$

The initial temperature distribution is supposed uniform

$$T = T_o \quad \text{for} \quad 0 < x < L \quad 0 < y < E_s \quad t = 0. \quad (11)$$

Fin temperature distribution

The following partial differential equation can be derived by writing the energy balance of an element of the fin:

$$\rho_m C_m \frac{\partial T_m}{\partial t} = k_m \frac{\partial^2 T}{\partial y^2} + \frac{2h_c}{E_m}(T - T_m). \quad (12)$$

The boundary conditions are as follows:

$$\frac{\partial T_m}{\partial y} = 0 \quad \text{for} \quad y = 0 \quad t > 0 \quad (13)$$

$$T_m = T_\infty \quad \text{for} \quad y = E_s \quad t > 0. \quad (14)$$

The initial fin temperature is also supposed uniform and equal to T_o,

$$T_m = T_o \quad \text{for} \quad 0 < y < E_s \quad t = 0. \quad (15)$$

The rate of sorption

For a nonuniform uptake distribution, the mass of the adsorbed phase at time t, $M_a(t)$, is obtained by integrating the uptake W over the volume of the adsorbent

$$M_a(t) = \rho_s \int_V W \, dV. \quad (16)$$

Introducing the average uptake $W_{avg}(t)$ defined as

$$W_{avg}(t) = \frac{1}{V}\int_V W \, dV \quad (17)$$

the expression of $M_a(t)$ becomes

$$M_a(t) = M_s W_{avg}(t). \quad (18)$$

Since the desorbed mass $m_{des}(t)$ between times 0 and t is equal to the change in the mass of the adsorbed phase, we have

$$m_{des}(t) = M_a(0) - M_a(t) = M_s[W_o - W_{avg}(t)]. \quad (19)$$

As the final equilibrium state characterized by uniform temperature T_∞ and uptake W_∞ is approached, the desorbed mass tends to its maximum value $m_{des}(\infty)$ given by

$$m_{des}(\infty) = M_a(0) - M_a(\infty) = M_s(W_o - W_\infty). \quad (20)$$

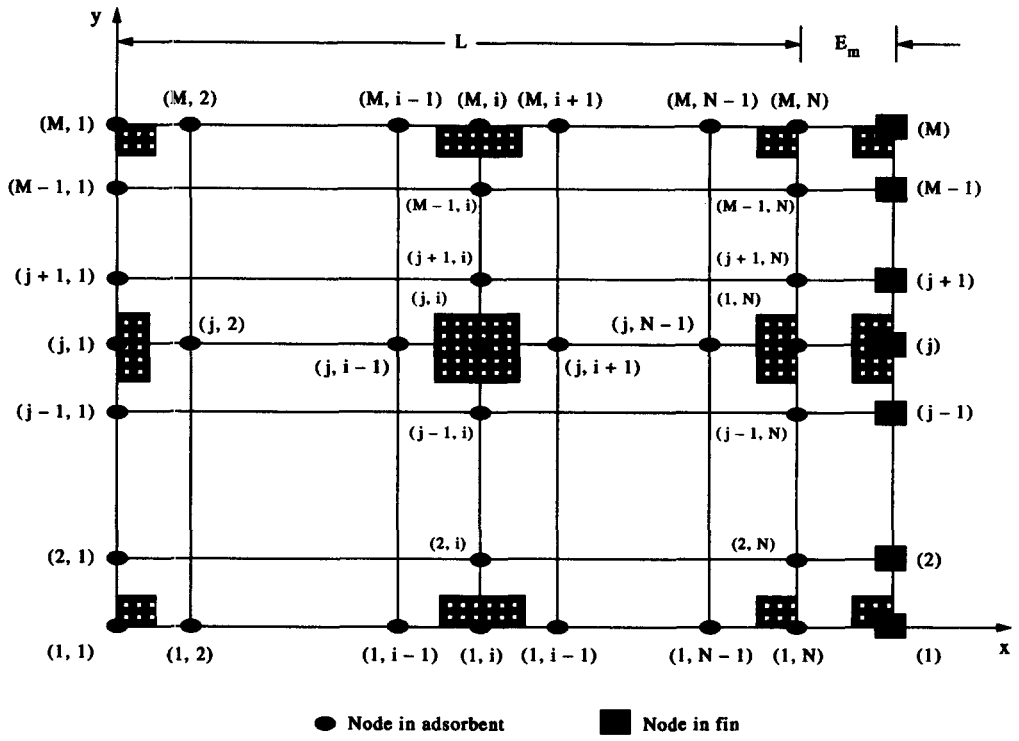

Fig. 4. The grid of the numerical solution.

The progress of the desorption process is measured by the ratio

$$R_{des}(t) = \frac{m_{des}(t)}{m_{des}(\infty)} = \frac{W_{avg}(t) - W_o}{W_\infty - W_o} \tag{21}$$

which is comprised between 0 and 1 and proportional to the desorbed mass. The rate of sorption $r_{des}(t)$ defined as the mass flow of desorbed mass per unit adsorbent mass is expressed by

$$r_{des}(t) = \frac{1}{M_s}\frac{dm_{des}(t)}{dt} = (W_o - W_\infty)\frac{dR_{des}(t)}{dt}. \tag{22}$$

NUMERICAL SOLUTION

Figure 4 shows the grid used to obtain the numerical solution. The adsorbent element is divided into $N-1$ divisions in the x-direction and $M-1$ in the y-direction. The fin is divided into $M-1$ elements. Applying heat balance equations to appropriate elementary volumes yields a finite difference form of the governing equations. In order to have an explicit scheme, the physical properties are supposed constant and evaluated at the previous iteration.

Finite difference form of the dimensionless governing equations

A convenient form of the finite difference equations is obtained by introducing the following dimensionless variables and parameters:

$$\theta = \frac{T - T_\infty}{T_0 - T_\infty} \quad \theta_m = \frac{T_m - T_\infty}{T_0 - T_\infty} \quad \xi = \frac{C_{ap}}{C_s} \quad \kappa = \frac{k}{k_s} \tag{23}$$

$$\zeta = \frac{x}{L} \quad \eta = \frac{y}{E_s} \quad \tau = \frac{t}{(\rho_s C_s/k_s)E_s^2} \tag{24}$$

$$\Delta\zeta = \frac{\Delta x}{L} = \frac{1}{N-1} \quad \Delta\eta = \frac{\Delta y}{E_s} = \frac{1}{M-1}$$

$$\Delta\tau = \frac{(k_s/\rho_s C_s)\Delta t}{E_s^2} \tag{25}$$

$$C_1 = \frac{\Delta\tau}{(\Delta\eta)^2} \quad C_2 = \left(\frac{E_s}{L}\frac{\Delta\eta}{\Delta\zeta}\right)^2 \quad C_3 = \frac{h_c E_s}{k_s} \tag{26}$$

$$C_4 = \frac{h_c \Delta y}{k_s} = C_3\Delta\eta \quad C_5 = \frac{h_c(\Delta y)^2}{k_s \Delta x} = \frac{E_s}{L}\frac{(\Delta\eta)^2}{\Delta\zeta}C_3 \tag{27}$$

$$C_6 = \frac{k_m/\rho_m C_m}{k_s/\rho_s C_s}\frac{\Delta\tau}{(\Delta\eta)^2} \quad C_7 = \frac{h_c(\Delta y)^2}{k_m E_m} = \frac{k_s}{k_m}\frac{E_s}{E_m}(\Delta\eta)^2. \tag{28}$$

The governing equations become

In the adsorbent matrix

$1 < j < M$ and $1 < i < N$

$$\theta_{j,i}^{p+1} = \frac{\kappa_{j,i}^{p}}{\xi_{j,i}^{p}} C_1 [C_2(\theta_{j,i+1}^{p} + \theta_{j,i-1}^{p} + \theta_{j+1,i}^{p} + \theta_{j-1,i}^{p}] + [1 - 2\frac{\kappa_{j,i}^{p}}{\xi_{j,i}^{p}} C_1(1+C_2)]\theta_{j,i}^{p} \quad (29)$$

$1 < j < M$ and $i = 1$

$$\theta_{j,1}^{p+1} = \frac{\kappa_{j,1}^{p}}{\xi_{j,1}^{p}} C_1 [2C_2\theta_{j,2}^{p} + \theta_{j+1,1}^{p} + \theta_{j-1,1}^{p}] + [1 - 2\frac{\kappa_{j,1}}{\xi_{j,1}^{p}} C_1(1+C_2)]\theta_{j,1}^{p} \quad (30)$$

$1 < j < M$ and $i = N$

$$\theta_{j,N}^{p+1} = \frac{\kappa_{j,N}^{p}}{\xi_{j,N}^{p}} C_1 [2C_2\theta_{j,N-1}^{p} + \theta_{j+1,N}^{p} + \theta_{j-1,N}^{p}] + \left[1 - 2\frac{\kappa_{i,N}}{\xi_{j,N}^{p}} C_1\left(1 + C_2 + \frac{C_5}{\kappa_{j,N}^{p}}\right)\right] \times \theta_{j,N}^{p} + 2\frac{C_1 C_5}{\xi_{j,N}^{p}}\theta_{m,j}^{p} \quad (31)$$

$j = M$ and $1 < i < L$

$$\theta_{M,1}^{p+1} = \frac{\kappa_{M,i}^{p}}{\xi_{M,i}^{p}} C_1 [C_2(\theta_{M,i-1}^{p} + \theta_{M,i+1}) + 2\theta_{M-1,i}^{p}] + \left[1 - 2\frac{\kappa_{M,i}}{\xi_{M,i}^{p}} C_1\left(1 + C_2 + \frac{C_4}{\kappa_{M,i}^{p}}\right)\right] \times \theta_{M,i}^{p} + 2\frac{C_1 C_4}{\xi_{M,i}^{p}}\theta_{\infty} \quad (32)$$

$j = M$ and $i = 1$

$$\theta_{M,1}^{p+1} = 2\frac{\kappa_{M,1}^{p}}{\xi_{M,i}^{p}} C_1 [C_2\theta_{M,2}^{p} + \theta_{M-1,1}^{p}] + \left[1 - 2\frac{\kappa_{M,1}}{\xi_{M,1}^{p}} C_1\left(1 + C_2 + \frac{C_4}{\kappa_{M,1}^{p}}\right)\right] \times \theta_{M,1}^{p} + 2\frac{C_1 C_4}{\xi_{M,1}^{p}}\theta_{\infty} \quad (33)$$

$j = M$ and $i = N$

$$\theta_{M,N}^{p+1} = 2\frac{\kappa_{M,N}^{p}}{\xi_{M,N}^{p}} C_1 (C_2\theta_{M,N-1}^{p} + \theta_{M-1,N}^{p}) + \left[1 - 2\frac{\kappa_{M,N}^{p}}{\xi_{M,N}^{p}} C_1\left(1 + C_2 + \frac{C_4 + C_5}{\kappa_{M,N}^{p}}\right)\right]\theta_{M,N}^{p} + \frac{2C_1(C_4 + C_5)}{\xi_{M,N}^{p}}\theta_{m,M}^{p} \quad (34)$$

$j = 1$ and $i = 1$

$$\theta_{1,1}^{p+1} = 2\frac{\kappa_{1,1}^{p}}{\xi_{1,1}^{p}} C_1 [C_2\theta_{1,2}^{p} + \theta_{2,1}^{p}] + \left[1 - 2\frac{\kappa_{1,1}}{\xi_{1,1}^{p}} C_1(1+C_2)\right]\theta_{1,1}^{p} \quad (35)$$

$j = 1$ and $1 < i < N$

$$\theta_{1,i}^{p+1} = \frac{\kappa_{1,i}^{p}}{\xi_{1,i}^{p}} C_1 [C_2(\theta_{1,i+1}^{p} + \theta_{1,i-1}^{p}) + 2\theta_{2,i}^{p}] + \left[1 - 2\frac{\kappa_{1,i}}{\xi_{1,i}^{p}} C_1(1+C_2)\right]\theta_{1,i}^{p} \quad (36)$$

$j = 1$ and $i = N$

$$\theta_{1,N}^{p+1} = 2\frac{\kappa_{1,N}^{p}}{\xi_{1,N}^{p}} C_1 (C_2\theta_{1,N-1}^{p} + \theta_{2,N}^{p}) + \left[1 - \frac{2C_1\kappa_{l,N}}{\xi_{j,N}^{p}}\left(1 + C_2 + \frac{C_5}{\kappa_{1,N}^{p}}\right)\right] \times \theta_{1,N}^{p} + 2\frac{C_1 C_5}{\xi_{1,N}^{p}}\theta_{m,1}^{p} \quad (37)$$

In the fin

$1 < j < n$

$$\theta_{m,j}^{p+1} = [1 - 2C_6(1+C_7)]\theta_{m,j}^{p} + C_6(2C_7\theta_{j,N}^{p} + \theta_{m,j-1}^{p} + \theta_{m,j+1}^{p}) \quad (38)$$

$j = 1$

$$\theta_{m,1}^{p+1} = [1 - 2C_6(1+C_7)]\theta_{m,1}^{p} + 2C_6(C_7\theta_{1,N}^{p} + \theta_{m,2}^{p}) \quad (39)$$

$j = M$

$$\theta_{m,M}^{p+1} = 1. \quad (40)$$

Convergence conditions

In order to avoid divergence and instability of the numerical solution, we make sure that the coefficients appearing in the finite difference equations are positive by imposing on the time and space steps the following conditions:

$$1 - 2\frac{\kappa_{j,i}^{p}}{\xi_{j,i}^{p}} C_1\left(1 + C_2 + \frac{C_4 + C_5}{\kappa_{M,i}}\right) \geqslant 0 \quad (41)$$

and

$$1 - 2C_6(1+C_7) \geqslant 0. \quad (42)$$

These conditions are used to calculate the time step when the space steps are fixed

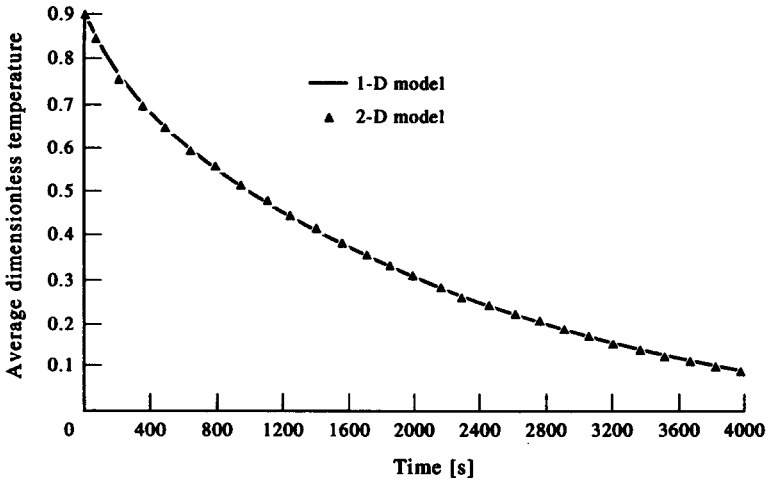

Fig. 5. Validation of the numerical solution by comparison to the non finned reactor. Case of a large distance between the fins.

$$\Delta\tau = \min\left[\frac{\min(\xi)(\Delta\eta)^2}{2[\max(\kappa)(1+C_2)+C_4+C_5]}\right.$$

$$\left.\frac{(k_s/\rho_s C_s)(\Delta\eta)^2}{2(k_m/\rho_m C_m)(1+C_7)}\right]. \quad (43)$$

Organization of the computer program

A computer program is developed based on the above explicit numerical scheme. The program calculates at every time step the spacial temperature and uptake distributions as well as their average values. It also calculates instantaneous and cumulative values of the desorbed/adsorbed mass and various heat transfer quantities involved in the system energy analysis. The program calculates also the system cooling/heating coefficients of performance. The temperature distribution is determined at each time step, using the values at the previous iteration. The uptake distribution is then calculated from the isotherm equation. The average temperature and uptake and various energy quantities needed to evaluate the system performance are calculated by numerical integration. The physical properties (thermal conductivity and specific heat) are evaluated using the temperature distribution at the previous iteration.

Validation of the numerical solution

The numerical solution is validated by comparison with the solution obtained in ref. [10] for the case of a nonfinned reactor. This is done by taking either a large distance between the fins or a high contact resistance between the fin and the adsorbent so that the fin effect can be neglected. Figures 5 and 6 show that in both cases, the two solutions give close results.

RESULTS AND DISCUSSION

The computer program is used to analyze the influence of various design parameters on the kinetics of sorption, including the distance between the fins, the fin thickness and thermal conductivity and the contact resistance between metallic parts and the adsorbent material. The adsorption pair used in this study is Zeolite 4A-water. The other parameters are summarized in Table 1.

Figures 7 and 8 show that the distance between the fins has a strong effect on the sorption kinetics. The duration of a heating phase (half-time of a cooling/heating adsorption cycle) decreases from 30 min for a nonfinned reactor to 4 min only when fins are used at 5 mm interval. It is also seen that the fin effect is

Table 1. Input data and the output results

Parameter	Value	Unit
Adsorbent:		
Nature	Zeolite 4A	
Mass density	735.0	kg m^{-3}
Specific heat	836	J kg^{-1} K^{-1}
Thermal conductivity	0.2	W K^{-1} m
Thickness	10/variable	mm
Adsorbate:		
Nature	Water	
Specific heat	4180	J kg^{-1} K^{-1}
Thermal conductivity	0.6	W K^{-1} m
Fin characteristics:		
Nature	Copper/variable	
Mass density	8133	kg m^{-3}
Specific heat	385	J kg^{-1} K^{-1}
Thermal conductivity	400	W K^{-1} m^{-1}
Thickness	1/variable	mm
Distance between fins	10/variable	mm
Contact resistance	10^{-5}/variable	m^2 K W^{-1}
Operating conditions:		
Condensation temperature	37.8	°C
Heating fluid temperature	200	°C
Initial temperature	20	°C

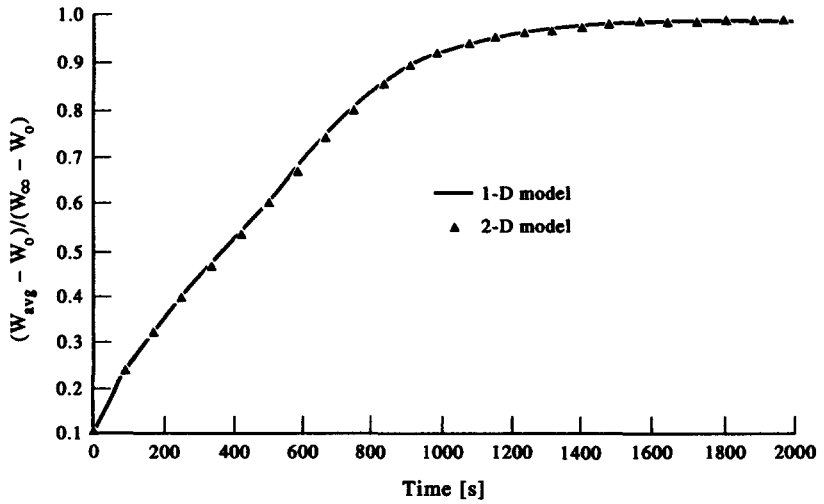

Fig. 6. Validation of the numerical solution by comparison to the non finned reactor. Case of an infinite contact resistance between fins and adsorbent.

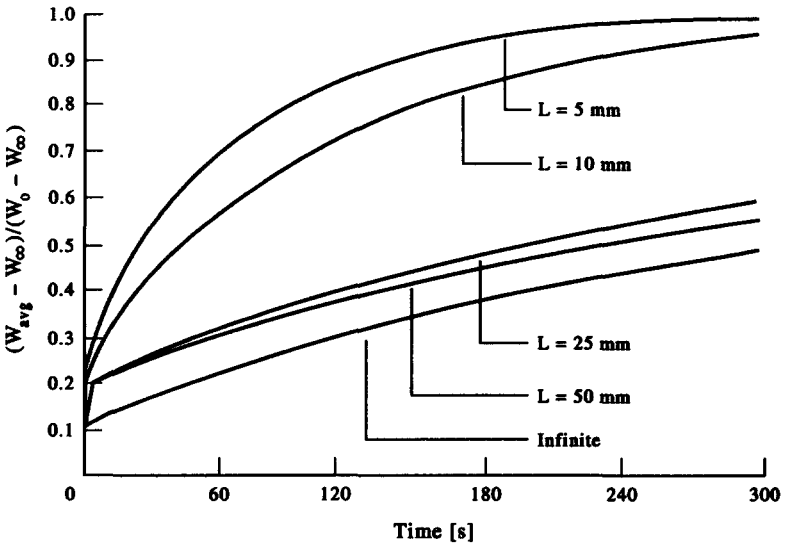

Fig. 7. Effect of the distance between the fins on sorption kinetics.

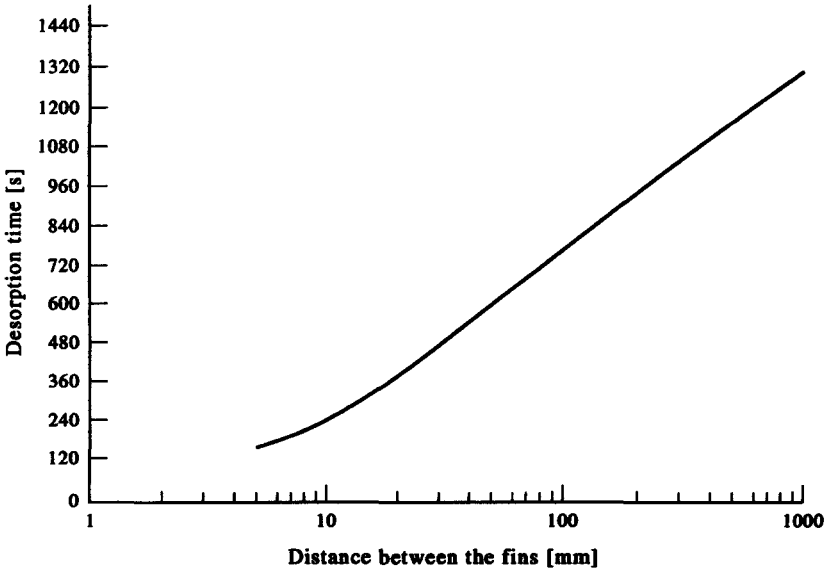

Fig. 8. Effect of the distance between the fins on the desorption time (time at which $R_{des} = 90\%$).

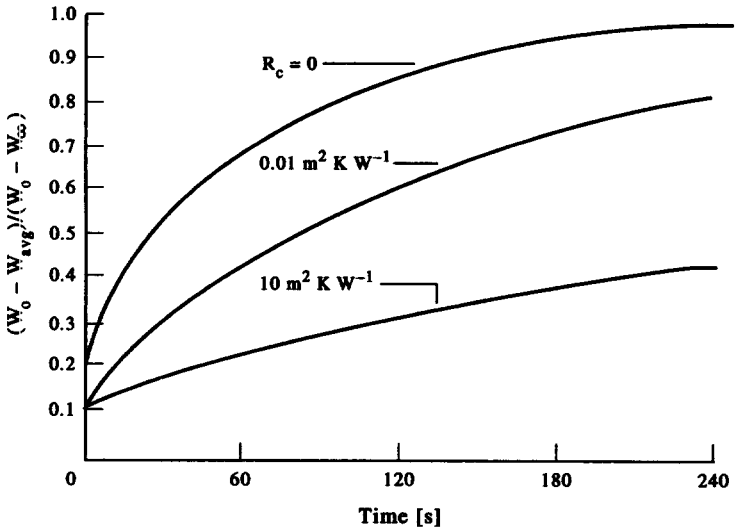

Fig. 9. Effect of the contact resistance at the interface metal-adsorbent on sorption kinetics.

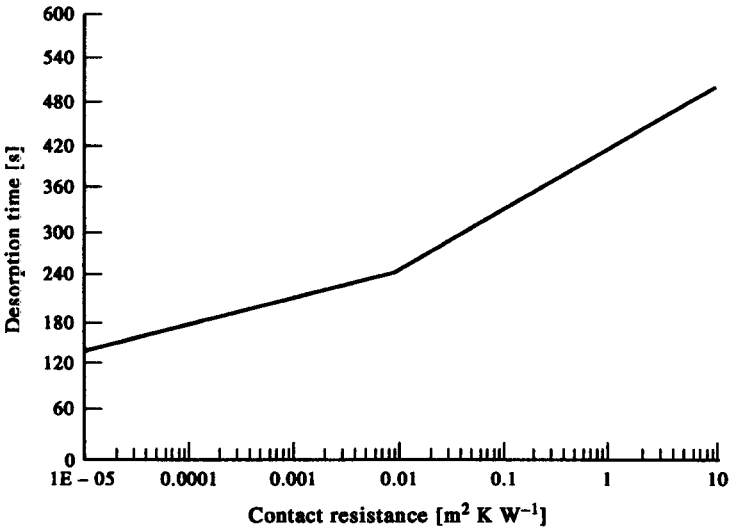

Fig. 10. Effect of the contact resistance at the interface metal-adsorbent on the desorption time (time at which $R_{des} = 90\%$).

negligible when the distance between the fins exceeds 50 mm.

Figures 9 and 10 show that the contact resistance between the adsorbent and metallic parts affects significantly the sorption kinetics. For a resistance of 10^{-5} m^2 K W^{-1}, the fin temperature is equal to that of the adsorbent in contact with the metal. We also notice no improvement of the heat transfer rate by the fins when the contact resistance increases to 10 m^2 K W^{-1}.

Figure 11 shows that the fin thickness has practically no effect on sorption kinetics. Desorption time remains unchanged when the fin thickness is varied from 0.1 to 1 mm. This shows that the low adsorbent thermal conductivity limits the rate of heat transfer between the fin and the adsorbent. A similar result is obtained when the nature of the metal is changed. No difference was found between fins made of copper, aluminum and steel.

CONCLUSIONS

A two-dimension model is developed to study sorption kinetics and the behavior of adsorption cooling systems with finned reactors. The governing equations derived from local energy balance and thermodynamic equilibrium are solved using an explicit numerical scheme. The solution is validated by comparison to previous results. The model is then used to evaluate the influence of various design parameters on sorption kinetics.

The parametric analysis revealed that a significant improvement of sorption kinetics can be obtained by

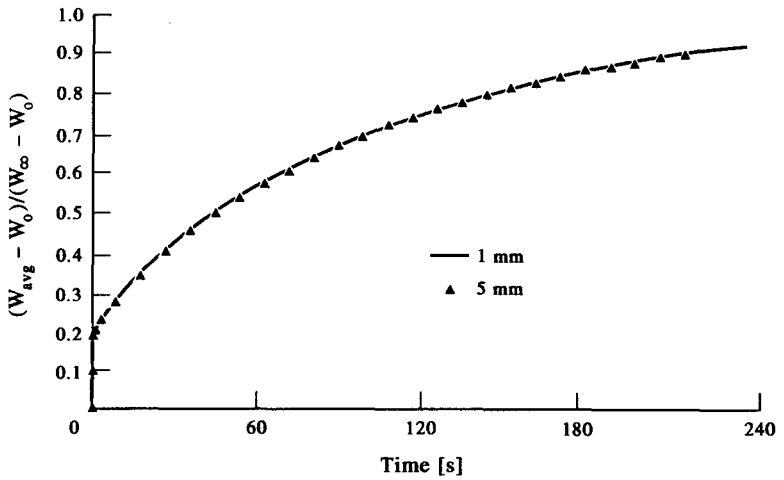

Fig. 11. Effect of the fin thickness on sorption kinetics.

reducing the distance between the fins and the contact resistance at the interface metal-adsorbent. However, the thickness of the fin and the nature of the metal has very low effect on the improvement. Therefore thin fins and cheap metals are recommended if the price of the cost and weight of the system are to be minimized.

Acknowledgement—The lead author acknowledges the financial support of the IFS located in Stockholm, Sweden.

REFERENCES

1. M. Groll, Solid sorption machines for CFC-free generation of heat and cold : an overview, presented at the first *ISHMT-ASME Heat and Mass Transfer Conference*, Bombay, 5–7 January (1994).
2. A, Hajji, Analysis of combined and heat mass transfer in closed-cycle adsorption cooling and heating systems, Ph.D. Thesis, Illinois Institute of Technology, Chicago (1987).
3. R. E. Critoph and R. Vogel, Possible adsorption pairs for use in solar cooling, *Int. J. Ambient Energy* **7** (1986).
4. M. Suzuki, Application of adsorption cooling system to automobiles, *Proceedings of Commission B1 of the IIR*, Paris, 18–20 November 1992 (Edited by the International Institute of Refrigeration), pp. 154–159 (1992).
5. S. V. Shelton, Residential Space Conditioning with Solid Sorption Technology, *Proceedings of Commission B1 of the IIR*, Paris, 18–20 November 1992 (Edited by the International Institute of Refrigeration), pp. 67–76 (1992).
6. Anonymous, Solid sorption refrigeration, *Proceedings of Commission B1 of the IIR*, Paris, 18–20 November 1992 (Edited by the International Institute of Refrigeration) (1992).
7. N. Douss, F. E. Meunier and L. M. Sun, Predictive model and experimental results for a two-adsorber solid adsorption heat pump, *Ind. Engng Chem. Res.* **27,** 310–316 (1988).
8. A. Hajji and W. M. Worek, Simulation of regenerative closed-cycle adsorption cooling/heating system, *Energy* **16,** 643–654 (1991).
9. M. Groll, W. Supper, U. Mayer and O. Brost, Heat and mass transfer limitations in metal hydride reaction beds, *Int. J. Hydrogen Energy* **12,** 89–97 (1987).
10. A. Hajji and S. Khalloufi, Theoretical and experimental investigation of a constant-pressure adsorption process, *Int. J. Heat Mass Transfer* **38,** 3349–3358 (1995).
11. L. D. Kirol and U. Rockenfeller, Industrial heat pumps using complex compound sorption media, *Proceedings of the 1989 ASME Winter Annual Meeting* (1990).
12. Ph. Touzain and M. Moundanga-Iniamy, Utilization of magnesium chloride graphite intercalation compound ammonia couple in a solid-sorption system, *Proceedings of Commission B1 of the IIR*, Paris, 18–20 November 1992 (Edited by the International Institute of Refrigeration), pp. 185–190 (1992).
13. J-J. Guilleminot, J. M. Gurgel, Heat transfer intensification in adsorbent beds of adsorbtion thermal devices, *Proceedings of Commission B1 of the IIR*, Paris, 18–20 November 1992 (Edited by the International Institute of Refrigeration), pp. 233–238 (1992).
14. G. Crozat, Optimisation des surfaces d'échange dans les réacteurs de pompes à chaleur himiques, *Rev. générale Thermique* **341** (1990).
15. R. K. Strauss, Schallenberg and K. F. Knoche, Measurement of the kinetics of water vapor adsorption into solid Zeolite layers, *Proceedings of Commission B1 of the IIR*, Paris, 18–20 November 1992 (Edited by the International Institute of Refrigeration), pp. 246–250 (1992).
16. G. Cacciola, G. Cammarata, A. Fichera and G. Restuccia, Advances on innovative heat exchangers in adsorption heat pumps, *Proceedings of Commission B1 of the IIR*, Paris, 18–20 November 1992 (Edited by the International Institute of Refrigeration), pp. 239–245 (1992).
17. K. F. Knoche and R. Lang, Heat exchangers coated with Zeolite for adsorption heat pumps, paper presented at München Discussion Meeting, Center for Applied Energy (ZAE), Technical University of München, Germany (1994).
18. A. Hajji and W. Worek, Thermodynamic modeling of constant-volume and constant-pressure processes in closed-cycle adsorption cooling/heating systems, *Chem. Engng Commun.* **104,** 21–40 (1991).
19. A. Hajji, G. Cacciola and G. Restuccia, Experimental and theoretical study of a constant-volume adsorption process, *Energy* **19,** 961–965 (1994).